

$^{13}\text{C}$  NMR ( $\text{C}_6\text{D}_6$ , +23 °C) 198.9 (C-1), 149.2 (C-9), 141.1 (C-2), 137.5 (C-8), 133.6 (C-10), 124.1, 123.6, 123.5 (C-3, C-4, C-6), 122.3 (C-7), 57.5 (N-CH<sub>2</sub>), 46.2 (N-CH<sub>3</sub>), -11.7 (CH<sub>3</sub>Li).

**2D NMR Experiments.** The conditions for the 2D NMR measurements on the various samples are summarized in Table I. The pulse sequences were the following: COSY,  $90^\circ-t_1-90^\circ/45^\circ-t_2$ -delay;<sup>32</sup> C-H shift correlation,  $90^\circ(^1\text{H})-t_1/2-180^\circ(^{13}\text{C})-t_1/2-\Delta_1-90^\circ(^1\text{H})$ ,  $90^\circ(^{13}\text{C})-\Delta_2-t_2/2^1\text{H}$ -bb-decoupling-delay;<sup>21</sup>  $^6\text{Li}-^1\text{H}$  HOESY,  $90^\circ(^1\text{H})-t_1/2-180^\circ(^6\text{Li})-t_1/2-90^\circ(^1\text{H})-\tau-90^\circ(^6\text{Li})-t_2/2^1\text{H}$ -bb-decoupling-delay.<sup>5</sup> 2D plots are presented in the absolute value mode. The COSY data matrices were symmetrized after Fourier transformation. The  $^6\text{Li}-^1\text{H}$  HOESY experiments were run with  $90^\circ$  pulse lengths 31  $\mu\text{s}$

( $^6\text{Li}$ ) and 85  $\mu\text{s}$  ( $^1\text{H}$ ), respectively, and a pulse delay of 6 to 8 s. For each sample measured, several runs with varying mixing time,  $\tau$ , were taken. Optimal signal-to-noise ratio was obtained for  $\tau \sim 2$  s.

MNDO calculations<sup>33</sup> with parametrization for lithium<sup>34</sup> were carried out on a CYBER 845 and an IBM 4361 computer.

**Acknowledgment.** This work was supported by the Deutsche Forschungsgemeinschaft and the Fonds der Chemischen Industrie. We thank Dr. M. Feigel for helpful and stimulating discussions.

**Registry No.** 1-Lithionaphthalene, 14474-59-0.

(32) Bax, A.; Freeman, R. *J. Magn. Reson.* **1981**, *44*, 542.

(33) Dewar, M. J. S.; Thiel, W. *J. Am. Chem. Soc.* **1977**, *99*, 4899, 4907.

(34) Lithium parametrization: Thiel, W.; Clark, T., QCPE Newsletter, submitted. (See the MNDOC Program; Thiel, W. QCPE Program No. 438.)

## Theoretical Study of Hydridocobalt Carbonyls

Danko Antolovic and Ernest R. Davidson\*

Contribution from the Department of Chemistry, Indiana University, Bloomington, Indiana 47405. Received June 13, 1986

**Abstract:** The molecular geometry and electronic structure of hydridocobalt tri- and tetracarbonyls were investigated, by means of ab initio Hartree-Fock calculations in a Gaussian basis set. Two conformations of the tetracarbonyl were found, both having the  $d^8$ , closed-shell electronic configuration. The tricarbonyl complex was found to possess a number of conformations, as well as several low-energy electronic configurations. We examine the geometry, frontier orbitals, and character of chemical bonds of these forms of  $\text{HCo}(\text{CO})_4$  and  $\text{HCo}(\text{CO})_3$ , with the aim of determining their relevance to the catalytic activity of the compounds.

In this article we endeavor to study the molecular geometry and electronic structure of hydridocobalt tri- and tetracarbonyls. Hydridocobalt tetracarbonyl is a well-known compound, of importance as catalyst in the hydroformylation process.<sup>1</sup> Tricarbonyl, on the other hand, is a largely hypothetical species. It is assumed to be the actual catalyst in the hydroformylation reaction, present in small amounts in the reaction mixture, due to spontaneous decomposition of the tetracarbonyl.

The molecular structure of the tetracarbonyl compound was determined by gas-phase electron diffraction experiments of McNeill and Scholer,<sup>2</sup> who found the molecule to have  $C_{3v}$  symmetry and an H-Co bond length of 1.556 Å.

There is only indirect evidence for the existence of  $\text{HCo}(\text{CO})_3$ . Ungvary and Marko<sup>3</sup> have carried out kinetic studies of the decomposition of  $\text{HCo}(\text{CO})_4$  into dicobalt octacarbonyl and hydrogen under the assumption that the establishment of an  $\text{HCo}(\text{CO})_4$ - $\text{HCo}(\text{CO})_3$  equilibrium is the first step in this reaction. Kinetic results are in agreement with this assumption, and the equilibrium constant corresponds to a concentration of  $\text{HCo}(\text{CO})_3$  equal to roughly 0.3% of the concentration of  $\text{HCo}(\text{CO})_4$  in *n*-heptane solution.

In a later study, Wermer et al.<sup>4a</sup> have reported evidence for  $\text{HCo}(\text{CO})_3$  in the IR spectra of the tetracarbonyl in an argon matrix at low temperature. They observed certain weak absorption bands whose intensity grew with irradiation of the sample and decreased in the presence of CO and which they could not assign to any known cobalt carbonyl. Their estimate is that the concentration of  $\text{HCo}(\text{CO})_3$  amounts to 0.2% of that of  $\text{HCo}(\text{CO})_4$ .

In an independent study of the photolysis of  $\text{HCo}(\text{CO})_4$  in the argon and carbon monoxide matrices, Sweany<sup>4b</sup> reinterprets the

observations made by Wermer et al.<sup>4a</sup> and assigns two of the mentioned IR bands to the species  $\text{Co}(\text{CO})_4$ . This study assigns only one IR band to  $\text{HCo}(\text{CO})_3$ .

To date, there are no experimental results concerning the molecular geometry or the electronic structure of the tricarbonyl compound.

Both of these compounds have been the subject of theoretical investigations involving a range of computational techniques (extended Hückel theory,<sup>5-7</sup> CNDO/2,<sup>8</sup> INDO/1,<sup>9</sup> SCF-LCAO-MO,<sup>8,10</sup> SCF-X $\alpha$ -SW<sup>11</sup>). All of these studies agree in depicting  $\text{HCo}(\text{CO})_4$  as a closed-shell,  $d^8$ -complex with  $C_{3v}$  symmetry. Details of the predicted geometry correspond qualitatively to those found experimentally. For the tricarbonyl compound, on the other hand, there is no such consensus: different computational methods vary on the subject of the relative stability of different conformations of this complex, as well as on the details of its electronic structure.

We find theoretically predicted geometries, as reported in the literature, rather inconclusive. Some optimizations are incomplete;<sup>8,10</sup> in other cases it is not clear whether the reported symmetry is the result of a full geometry optimization or an ad hoc constraint.<sup>6,8</sup> Finally, some semiempirical methods<sup>9,12</sup> have, in the authors' experience, yielded unphysical geometries and should not be relied upon too strongly.

(5) Pensak, D. A.; McKinney, R. J. *Inorg. Chem.* **1979**, *18*, 3407.

(6) Bellagamba, V.; Ercoli, R.; Gamba, A.; Suffritti, G. B. *J. Organomet. Chem.* **1980**, *190*, 381.

(7) Boudreaux, E. A. *Inorg. Chim. Acta* **1984**, *82*, 183.

(8) Grima, J. Ph.; Choplin, F.; Kaufmann, G. *J. Organomet. Chem.* **1977**, *129*, 221.

(9) Iberle, K. A.; Davidson, E. R., unpublished results.

(10) Fønnesbech, N.; Hjortkjaer, J.; Johansen, H. *Int. J. Quantum Chem.* **1977**, *12*, 95.

(11) Eyermann, C. J.; Chung-Phillips, A. *J. Am. Chem. Soc.* **1984**, *106*, 7437.

(12) Various INDO schemes, as implemented in the program ZINDO, written by M. Zerner.

(1) Orchin, M. *Acc. Chem. Res.* **1981**, *14*, 259.

(2) McNeill, E. A.; Scholer, F. R. *J. Am. Chem. Soc.* **1977**, *99*, 6243.

(3) Ungvary, F.; Marko, L. *J. Organomet. Chem.* **1969**, *20*, 205.

(4) (a) Wermer, P.; Ault, B. S.; Orchin, M. *J. Organomet. Chem.* **1978**, *162*, 189. (b) Sweany, R. L. *Inorg. Chem.* **1980**, *19*, 3512.

**Table I.** Bond Lengths (Å) and Angles (deg) of  $\text{HCo}(\text{CO})_4$ 

parameter	$C_{3v}$	$C_{2v}$	$C_{3v}$ (exptl <sup>2</sup> )
H-Co	1.71	1.59	1.556
Co-C <sub>ax</sub>	2.02	2.04	1.764
Co-C <sub>eq</sub>	1.96	1.95	1.818
C <sub>ax</sub> -O <sub>ax</sub>	1.12	1.12	1.141
C <sub>eq</sub> -O <sub>eq</sub>	1.13	1.13	1.141
H-Co-C <sub>ax</sub>	180.0	85.6	180.0
H-Co-C <sub>eq</sub>	83.8	113.8	80.3
C <sub>eq</sub> -Co-C <sub>eq</sub>	118.8	132.4	117.3
Co-C <sub>ax</sub> -O <sub>ax</sub>	180.0	171.2	180.0
Co-C <sub>eq</sub> -O <sub>eq</sub>	167.8	176.5	172.6

In this work, we give an account of an ab initio LCAO-MO treatment of these two compounds, with special emphasis on the question of geometry and electronic structure of the less well understood of the two species,  $\text{HCo}(\text{CO})_3$ .

### Computational Details

The question of choice of the appropriate basis set for a molecule involving transition-metal atom(s) has by now received ample attention: a good basis set must describe the core reasonably well, it must also contain split-valence and diffuse functions to overcome the bias toward a single free-atom configuration, and it must remain computationally accessible. Obviously, some compromises have to be made.

Our first objective is to obtain some information about the molecular geometry, by means of full geometry optimization at the SCF computational level. Therefore, we avoided heavily core-oriented basis sets,<sup>13,14</sup> such as have been proposed for calculations on transition-metal atoms. On the valence end, however, a very detailed description of the d-orbitals is also impracticable, since we wish to explore a fair number of different geometries.

As a working compromise, we have adopted the DZC basis set for cobalt, as proposed by Tatewaki and Huzinaga,<sup>15</sup> and augmented it with a set of diffuse<sup>16</sup> *p*-functions ( $\alpha = 0.085$ ), which amounts to a 12s7p4d basis, contracted as (33321/331/4). The standard 3-21 basis was used on the light atoms.

This basis is too small to give conclusive answers about the electronic structure but should be adequate for exploratory calculations. Calculations in a somewhat larger basis set are currently in progress, with the objective of elucidating some finer points of the structure.

Geometry optimizations were performed by means of the software package GAMESS on a Cyber 205, and subsequent single-point CI calculations were done with the program MELD on an FPS 164 array processor.

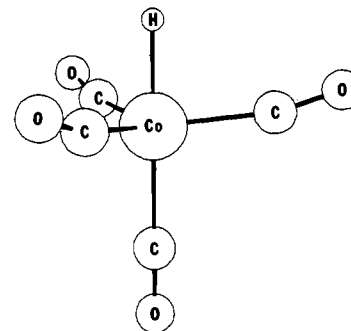
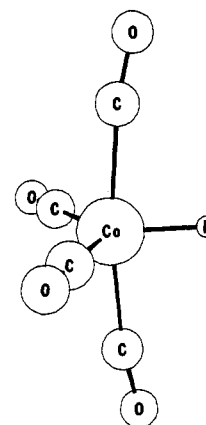
### Structure of the Tetracarbonyl Compound

There are at least three plausible geometries for  $\text{HCo}(\text{CO})_4$ : square pyramid ( $C_{4v}$ ), trigonal bipyramid ( $C_{3v}$ ), and distorted trigonal bipyramid with hydrogen in the equatorial position ( $C_{2v}$ ). The  $C_{3v}$  geometry is by far the most carefully described in the literature.

Electron diffraction results<sup>2</sup> are commonly invoked in favor of the  $C_{3v}$  structure, but it might be worth pointing out that both  $C_{3v}$  and  $C_{2v}$  geometries were compared with experimental results.  $C_{3v}$  fits the data much better, but the alternative geometry,  $C_{2v}$ , was not ruled out entirely.

Past theoretical studies<sup>6,8</sup> found the  $C_{3v}$  geometry more stable than  $C_{4v}$ , but no optimizations were done for the  $C_{2v}$  geometry. In an EHT study of transition-metal carbonyl fragments, Elian and Hoffmann<sup>18</sup> address all three possibilities and provide an elegant semiquantitative argument in favor of  $C_{3v}$ . We shall return to this argument later.

We have carried out full optimization of the  $C_{3v}$  and  $C_{2v}$  geometries of  $\text{HCo}(\text{CO})_4$  under the constraint of symmetry and assuming a closed-shell electron configuration. Results are listed in Table I. In both cases, the geometry can be regarded as a distorted trigonal bipyramid (TBP), with hydrogen in either apical or equatorial position and with carbonyl oxygens tilted slightly toward the hydrogen atom (see Figures 1 and 2).

**Figure 1.**  $C_{3v}$  conformation of  $\text{HCo}(\text{CO})_4$ ,  $^1A_1$ .**Figure 2.**  $C_{2v}$  conformation of  $\text{HCo}(\text{CO})_4$ ,  $^1A_1$ .**Table II.** Charge Distributions on  $\text{HCo}(\text{CO})_4$ 

atom	Mulliken		Löwdin	
	$C_{3v}$	$C_{2v}$	$C_{3v}$	$C_{2v}$
H	-0.258	-0.123	-0.261	-0.158
Co	+0.389	+0.318	-0.519	-0.543
C <sub>ax</sub>	+0.358	+0.399	+0.223	+0.220
O <sub>ax</sub>	-0.416	-0.433	-0.008	-0.022
C <sub>eq</sub>	+0.428	+0.386	+0.232	+0.201
O <sub>eq</sub>	-0.452	-0.450	-0.043	-0.048

**Table III.** Highest Occupied Orbitals of  $\text{HCo}(\text{CO})_4$ 

orbital	energy, au	main components of orbital	
		$C_{3v}^c$	$C_{2v}^d$
17a <sub>1</sub>	-0.3392	0.256 (H 1s) +0.197d <sub>z<sup>2</sup> +0.208 (Co s<sub>4</sub>) +0.124 (C<sub>ax</sub> 2s')</sub>	+0.482 (H 1s') +0.339 (Co p <sub>3z</sub> ) <sup>a</sup> -0.169 (C <sub>eq</sub> 2s')
12e	-0.3587	-0.840d <sub>xy</sub> <sup>b</sup> 0.727d <sub>x<sup>2</sup>-y<sup>2</sup> -0.400 (Co p<sub>3x</sub>)</sub>	-0.400 (Co p <sub>3y</sub> ) -0.727d <sub>y<sup>2</sup></sub>
11e	-0.4960	-0.949d <sub>xz</sub> +0.107d <sub>z<sup>2</sup> 0.949d<sub>yz</sub></sub>	-0.106d <sub>y<sup>2</sup> +0.123d<sub>xy</sub></sub>
19a <sub>1</sub>	-0.2775	-0.144 (H 1s) +0.452d <sub>x<sup>2</sup>-y<sup>2</sup> -0.586 (Co p<sub>3x</sub>)</sub>	-0.101 (H 1s') -0.474d <sub>y<sup>2</sup></sub>
18a <sub>1</sub>	-0.4091	-0.215 (H 1s) -0.587d <sub>x<sup>2</sup>-y<sup>2</sup> +0.190d<sub>z<sup>2</sup> -0.308 (Co s<sub>4</sub>)</sub></sub>	-0.451 (H 1s') +0.456d <sub>y<sup>2</sup> +0.172 (C<sub>ax</sub> 2s')</sub>
10b <sub>2</sub>	-0.4131	-0.893d <sub>xy</sub>	-0.332 (Co p <sub>3y</sub> )
10b <sub>1</sub>	-0.5041	0.964d <sub>xz</sub>	
3a <sub>2</sub>	-0.5153	-0.944d <sub>yz</sub>	

<sup>a</sup> Fourth shell of the cobalt atom. <sup>b</sup> Members of the 6-fold Cartesian Gaussian set. <sup>c</sup> Total energy is -1824.6297 au. <sup>d</sup> Total energy is -1824.6318 au.

A separate optimization of the  $C_{3v}$  geometry, without any symmetry constraints, was also carried out, in order to check for

(13) Roos, B.; Veillard, A.; Vinot, G.; *Theor. Chim. Acta* **1971**, *20*, 1.

(14) Hyla-Kryspin, I.; Demuyne, J.; Strich, A.; Benard, M. *J. Chem. Phys.* **1981**, *75*, 3954.

(15) Tatewaki, H.; Huzinaga, S.; *J. Chem. Phys.* **1979**, *71*, 4339.

(16) *Gaussian Basis Sets for Molecular Calculations*; Huzinaga, S., Ed.; Elsevier: Amsterdam, 1984; p 24.

**Table IV.** Bond Lengths (Å) and Angles (deg) of the Closed-Shell Configurations of HCo(CO)<sub>3</sub>

parameter	HV (C <sub>3v</sub> )	HC (C <sub>s</sub> )	CC (C <sub>s</sub> )	CV (C <sub>s</sub> )
H-Co	1.71	1.71	1.63	1.61
Co-C <sub>ax</sub>		1.97	1.99	2.02
Co-C <sub>eq</sub>	1.97	1.93	1.85	1.96
C <sub>ax</sub> -O <sub>ax</sub>		1.12	1.12	1.12
C <sub>eq</sub> -O <sub>eq</sub>	1.13	1.12	1.13	1.13
H-Co-C <sub>ax</sub>		163.6	87.4	96.6
H-Co-C <sub>eq</sub>	89.7	87.9	136.3	115.7
C <sub>eq</sub> -Co-C <sub>eq</sub>	120.0	133.4		125.6
Co-C <sub>ax</sub> -O <sub>ax</sub>		178.3	172.2	173.4
Co-C <sub>eq</sub> -O <sub>eq</sub>	166.8	163.4	161.0	176.6
C <sub>ax</sub> -Co-C <sub>ax</sub>			164.4	

**Table V.** Mulliken Charge Distribution on the Closed-Shell Configurations of HCo(CO)<sub>3</sub>

atom	HV (C <sub>3v</sub> )	HC (C <sub>s</sub> )	CC (C <sub>s</sub> )	CV (C <sub>s</sub> )
H	-0.316	-0.269	-0.250	-0.141
Co	+0.425	+0.489	+0.512	+0.334
C <sub>ax</sub>		+0.327	+0.299	+0.372
O <sub>ax</sub>		-0.416	-0.452	-0.424
C <sub>eq</sub>	+0.401	+0.376	+0.379	+0.370
O <sub>eq</sub>	-0.437	-0.441	-0.434	-0.441

possible second-order Jahn-Teller distortions. Within the accuracy of the optimization, none were found.

**Table VI.** Frontier Orbitals of the Closed-Shell Configurations of HCo(CO)<sub>3</sub>

orbital	occupation	energy, au	main components of orbital		orbital	occupation	energy, au	main components of orbital	
HV (C <sub>3v</sub> ) <sup>a</sup>									
13a <sub>1</sub>	0	+0.0464	-0.303 (H 1s')	-0.176d <sub>z2</sub>				-0.118 (C <sub>eq</sub> 2p <sub>x</sub> )	+0.133 (C <sub>eq</sub> 2p' <sub>y</sub> )
			+0.312 (Co s <sub>4</sub> )	-0.974 (Co s <sub>5</sub> )				+0.115 (O <sub>eq</sub> 2p <sub>x</sub> )	+0.176 (O <sub>eq</sub> 2pμ <sub>x</sub> )
			+0.639 (Co p <sub>3z</sub> )					+0.149 (C <sub>ax</sub> , 2p <sub>y</sub> )	
			+0.264 (C 2s')	-0.128 (O 2p <sub>z</sub> )				-0.134 (C <sub>ax</sub> 2s')	+0.210 (C <sub>ax</sub> 2p' <sub>y</sub> )
12a <sub>1</sub>	2	-0.3339	0.256 (H 1s)	+0.507 (H 1s')	23a'	2	-0.3014	-0.137 (O <sub>ax</sub> 2p <sub>y</sub> )	-0.215 (O <sub>ax</sub> 2p' <sub>y</sub> )
			+0.161d <sub>z2</sub>					0.172 (H 1s)	+0.175 (H 1s')
			+0.268 (Co s <sub>4</sub> )	+0.246 (Co p <sub>3z</sub> )				+0.443d <sub>z2</sub>	-0.331d <sub>x2</sub>
			-0.159 (C 2s')					+0.361d <sub>xy</sub>	+0.138 (Co s <sub>4</sub> )
11e	2	-0.3549	-0.506d <sub>x2</sub>	+0.506d <sub>y2</sub>				+0.121 (Co p <sub>3y</sub> )	+0.484 (Co p <sub>3x</sub> )
			-0.618d <sub>xy</sub>		22a'	2	-0.3723	-0.114 (C <sub>ax</sub> 2s')	
			+0.258 (Co p <sub>3x</sub> )	-0.273 (Co p <sub>3y</sub> )				-0.135 (H 1s)	-0.299 (H 1s')
			0.535d <sub>x2</sub>	-0.535d <sub>y2</sub>				-0.179d <sub>x2</sub>	+0.309d <sub>z2</sub>
			-0.584d <sub>xy</sub>					+0.747d <sub>xy</sub>	
			+0.273 (Co p <sub>3x</sub> )	-0.258 (Co p <sub>3y</sub> )				-0.384 (Co s <sub>4</sub> )	+0.115 (Co p <sub>3x</sub> )
10e	2	-0.5008	0.746d <sub>xz</sub>	-0.624d <sub>yz</sub>	21a'	2	-0.3837	+0.147 (C <sub>ax</sub> 2s')	
			-0.624d <sub>xz</sub>	-0.746d <sub>yz</sub>				-0.141 (H 1s)	-0.389 (H 1s')
								+0.732d <sub>z2</sub>	-0.574d <sub>x2</sub>
								-0.184d <sub>z2</sub>	-0.291d <sub>xy</sub>
								+0.179 (Co s <sub>4</sub> )	
24a'	0	+0.0365	-0.109 (H 1s')					-0.116 (C <sub>eq</sub> 2p' <sub>y</sub> )	-0.129 (O <sub>eq</sub> 2p' <sub>x</sub> )
			+0.138d <sub>x2</sub>	-0.114d <sub>z2</sub>	12a''	2	-0.4226	0.895d <sub>yz</sub>	-0.323d <sub>xz</sub>
			-0.135 (Co s <sub>4</sub> )	+0.288 (Co s <sub>5</sub> )	11a''	2	-0.4691	0.286d <sub>yz</sub>	+0.897d <sub>xz</sub>
			+0.586 (Co p <sub>3x</sub> )	-0.113 (Co p <sub>3z</sub> )					
			-0.133 (C <sub>ax</sub> 2s')						
			+0.198 (C <sub>ax</sub> 2p <sub>x</sub> )	+0.302 (C <sub>ax</sub> , 2p' <sub>x</sub> )	24a'	0	+0.0624	0.137 (H 1s')	
			-0.173 (O <sub>ax</sub> 2p <sub>x</sub> )	-0.275 (O <sub>ax</sub> 2p' <sub>x</sub> )				-0.174d <sub>z2</sub>	+0.146d <sub>x2</sub>
			+0.106 (C <sub>eq</sub> 2p <sub>x</sub> )	+0.161 (C <sub>eq</sub> 2p' <sub>x</sub> )				+0.132 (Co s <sub>4</sub> )	-0.379 (Co s <sub>5</sub> )
			-0.144 (O <sub>eq</sub> 2p' <sub>x</sub> )					+0.737 (Co p <sub>3z</sub> )	+0.113 (Co p <sub>3x</sub> )
23a'	2	-0.3274	-0.250 (H 1s)	-0.467 (H 1s')				-0.333 (C <sub>ax</sub> 2s')	+0.211 (C <sub>ax</sub> 2p <sub>z</sub> )
			+0.198d <sub>x2</sub>	-0.208d <sub>z2</sub>				+0.184 (C <sub>eq</sub> 2p <sub>z</sub> )	
			+0.124d <sub>xz</sub>	-0.332 (Co p <sub>3z</sub> )				+0.180 (C <sub>eq</sub> 2s')	+0.237 (C <sub>eq</sub> 2p' <sub>z</sub> )
			+0.156 (C <sub>eq</sub> 2s')					-0.161 (O <sub>eq</sub> 2p <sub>z</sub> )	-0.249 (O <sub>eq</sub> 2p' <sub>z</sub> )
12a''	2	-0.3422	-0.865d <sub>xy</sub>	+0.113d <sub>yz</sub>	23a'	2	-0.2846	0.157 (H 1s)	+0.124 (H 1s')
			-0.383 (Co p <sub>3y</sub> )					-0.436d <sub>x2</sub>	+0.477d <sub>y2</sub>
22a'	2	-0.3711	-0.851d <sub>x2</sub>	+0.655d <sub>y2</sub>				+0.552 (Co p <sub>3x</sub> )	
			+0.268d <sub>z2</sub>	-0.425 (Co s <sub>4</sub> )	12a''	2	-0.4028	0.124d <sub>yz</sub>	+0.883d <sub>xy</sub>
			+0.112 (C <sub>ax</sub> 2s')					+0.317 (Co p <sub>3y</sub> )	
21a'	2	-0.4332	-0.139 (H 1s')	-0.952d <sub>xz</sub>	22a'	2	-0.4053	-0.205 (H 1s)	-0.435 (H 1s')
11a''	2	-0.4697	-0.164d <sub>xy</sub>	-0.932d <sub>yz</sub>				-0.574d <sub>x2</sub>	+0.533d <sub>z2</sub>
								-0.275 (Co s <sub>4</sub> )	+0.164 (C <sub>ax</sub> 2s')
								-0.945d <sub>yz</sub>	+0.150d <sub>xy</sub>
24a'	0	+0.0379	0.112d <sub>z2</sub>		11a''	2	-0.5150	0.963d <sub>xz</sub>	
			-0.151 (Co s <sub>4</sub> )	+0.412 (Co s <sub>5</sub> )	21a''	2	-0.5163		
			+0.592 (Co p <sub>3y</sub> )	-0.129 (Co p <sub>3x</sub> )					

<sup>a</sup> Total energy is -1712.4989 au. <sup>b</sup> Total energy is -1712.5023 au. <sup>c</sup> Total energy is -1712.5018 au. <sup>d</sup> Total energy is -1712.5089 au.

No separate optimization was performed for the C<sub>4v</sub> symmetry (square pyramid), but the C<sub>2v</sub>-constrained optimization did not show any signs of advancing toward a C<sub>4v</sub> configuration. Therefore, we shall limit the discussion to the former two geometries.

Tables I-III summarize the results of RHF-SCF calculations for HCo(CO)<sub>4</sub>. In Table III are given the energies and salient features of the highest occupied orbitals, which consist mostly of the cobalt d-orbitals and the H-Co bond.

The labels of the basis functions on the cobalt atom are those of Tatewaki and Huzinaga,<sup>15</sup> p<sub>3</sub> being the additional, diffuse p-shell. Functions s<sub>5</sub> and p<sub>3</sub> correspond approximately to the fourth sp-shell of the cobalt atom.

All of the d-functions listed in Tables III, VI, X, XIV, and XVIII belong to the 6-fold Cartesian Gaussian set. We find this choice more convenient than that of the canonical 5-fold spherical harmonics, since the d-orbitals on cobalt are heavily hybridized and differ considerably from the canonical d-orbitals. Even though this set is not purely d in character, the s-type combination, d<sub>x<sup>2</sup>+y<sup>2</sup>+z<sup>2</sup></sub>, was not found to contribute significantly to the molecular orbitals.

In the description of both conformations, the TBP axis lies along the z axis of the coordinate system, with one equatorial ligand placed in the xz plane. Hydrogen atom points in the positive z or x direction. We follow this convention throughout the article.

It can be seen from Table I that the carbonyl ligands can be classified as axial or equatorial (with respect to TBP) and that corresponding bond lengths have essentially the same value in both

**Table VII.** Bond Lengths (Å) and Angles (deg) of the  $^3A'$  Configurations of  $\text{HCo}(\text{CO})_3$ 

parameter	HC ( $C_2$ )	CC ( $C_2$ )
H-Co	1.64	1.64
Co-C <sub>ax</sub>	1.97	1.98
Co-C <sub>eq</sub>	2.12	2.14
C <sub>ax</sub> -O <sub>ax</sub>	1.15	1.13
C <sub>eq</sub> -O <sub>eq</sub>	1.12	1.13
H-Co-C <sub>ax</sub>	163.0	90.7
H-Co-C <sub>eq</sub>	87.5	121.0
C <sub>ax</sub> -Co-C <sub>ax</sub>		170.9
C <sub>eq</sub> -Co-C <sub>eq</sub>	138.5	
Co-C <sub>ax</sub> -O <sub>ax</sub>	177.2	170.4
Co-C <sub>eq</sub> -O <sub>eq</sub>	163.9	172.9

**Table VIII.** Mulliken Charge Distribution on the  $^3A'$  Configurations of  $\text{HCo}(\text{CO})_3$ 

atom	HC ( $C_2$ )	CC ( $C_2$ )
H	-0.253	-0.250
Co	+0.593	+0.415
C <sub>ax</sub>	+0.105	+0.370
O <sub>ax</sub>	-0.484	-0.433
C <sub>eq</sub>	+0.429	+0.384
O <sub>eq</sub>	-0.410	-0.423

conformations. Equatorial bonds are shorter than the axial ones; this is especially true for the H-Co bond, which is shorter by 0.12 Å in the equatorial position ( $C_{2v}$ ). This difference is accompanied by a difference in charge on the hydrogen atom (see Table II).

The d-orbital picture in both geometries corresponds to the pattern of the regular TBP structures of  $D_{3h}$  symmetry.<sup>18</sup> There is a low-lying  $e'$ -set, facing the sides of the bipyramid; an  $e'$ -set of equatorially oriented d-orbitals; and an axially oriented orbital at high energy. The orbitals of the  $e'$ -set hybridize strongly with 4p-orbitals of the metal atom, in order to avoid the equatorial ligands.

In the case of the  $C_{3v}$  conformation, the axial  $d_{z^2}$ -orbital participates in an spd-hybrid, forming the bond to hydrogen. The same orbital,  $17a_1$ , also has a modest bonding character with respect to the axial carbonyl.

It is interesting to point out that the  $e''$ -like orbitals of the  $C_{3v}$  conformation hybridize slightly with those of the equatorial set. This hybridization corresponds to the tilt of the equatorial carbonyls toward hydrogen and would, in case of the full-fledged  $T_d$  geometry, produce orbitals of the  $e$ -symmetry, facing the edges of the tetrahedron. More prominent orbitals of this kind are present in the tetrahedral forms of  $\text{HCo}(\text{CO})_3$ .

We notice that the orbital energy levels of the  $C_{2v}$  conformation correspond to those of a somewhat perturbed  $D_{3h}$  symmetry:  $3a_2$  and  $10b_1$  correspond to the  $e''$ -level and  $10b_2$  and  $18a_1$  to the  $e'$ -level in the  $D_{3h}$ . Another possible distortion, that of the  $C_{4v}$  symmetry, with the 4-fold axis in the  $x$  direction, would require a near degeneracy of the orbitals  $10b_1$  and  $10b_2$ . These two orbitals are separated by an energy gap of 0.091 au.

Also, formation of the H-Co bond in the  $C_{2v}$  case is superimposed onto the hybridization of the  $e'$ -set with metal 4p-orbitals. One of the  $e'$ -like orbitals,  $d_{x^2-y^2}$ , hybridizes with the cobalt 4s and forms the metal-hydrogen bonding orbital,  $18a_1$ , lower in energy than the corresponding bond orbital in the  $C_{3v}$  configuration. This tallies well with the shorter bond length for equatorial hydrogen (see Table I).

The antibonding combination,  $19a_1$ , on the other hand, hybridizes with a 4p-orbital and points away from the hydrogen. Thus,  $19a_1$  and  $10b_2$  resemble closely the  $e'$  equatorial pair, even though  $18a_1$  is closer to  $10b_2$  in energy than  $19a_1$ .

Finally, the  $C_{2v}$  configuration turns out to have an energy margin of 0.002 au over the  $C_{3v}$ . This runs contrary to the experimental findings and must not be treated as a conclusive result. However, we do wish to compare these results with earlier theoretical predictions about the geometry of  $\text{HCo}(\text{CO})_4$ .

**Population Analyses and Atomic Charges.** Some comments are in order concerning the significance of atomic charges obtained

**Table IX.** Mulliken Spin Population on the  $^3A'$  Configurations of  $\text{HCo}(\text{CO})_3$ 

atom	HC ( $C_2$ )	CC ( $C_2$ )
H	-0.002	-0.004
Co	1.429	1.789
C <sub>ax</sub>	0.343	0.038
O <sub>ax</sub>	0.148	0.027
C <sub>eq</sub>	0.025	0.059
O <sub>eq</sub>	0.016	0.027

**Table X.** Frontier Orbitals of the  $^3A'$  Configurations of  $\text{HCo}(\text{CO})_3$ 

orbital	occu- pation	energy, au	main components of orbital	
HC ( $C_2$ ) <sup>a</sup>				
24a'	1	-0.2092	-0.180d <sub>z<sup>2</sup></sub> +0.552 (Co p <sub>3x</sub> ) +0.278 (C <sub>ax</sub> 2p <sub>x</sub> ) -0.232 (O <sub>ax</sub> 2p <sub>x</sub> )	+0.165d <sub>y<sup>2</sup></sub>   +0.404 (C <sub>ax</sub> 2p' <sub>x</sub> ) -0.356 (O <sub>ax</sub> 2p' <sub>x</sub> )
23a'	1	-0.6231	0.960d <sub>x<sup>2</sup></sub> -0.601d <sub>y<sup>2</sup></sub> +0.199 (Co s <sub>4</sub> )	-0.396d <sub>z<sup>2</sup></sub>   +0.464 (H 1s')
22a'	2	-0.3794	0.264 (H 1s) +0.209d <sub>z<sup>2</sup></sub> +0.217 (Co s <sub>4</sub> ) -0.158 (C <sub>eq</sub> 2s')	-0.152d <sub>y<sup>2</sup></sub>   +0.295 (Co p <sub>3z</sub> )
12a''	2	-0.5500	0.803d <sub>xy</sub> +0.153 (Co p <sub>3y</sub> )	-0.219d <sub>yz</sub> -0.173 (C <sub>eq</sub> 2s')
21a'	2	-0.5694	-0.777d <sub>xz</sub> -0.197 (C <sub>ax</sub> 2p <sub>z</sub> ) -0.116 (C <sub>ax</sub> 2p' <sub>z</sub> )	-0.277 (C <sub>ax</sub> 2s') +0.128 (C <sub>eq</sub> 2s')
10a''	2	-0.6234	-0.804d <sub>yz</sub> +0.145 (C <sub>ax</sub> 2p <sub>y</sub> ) +0.206 (O <sub>ax</sub> 2p <sub>y</sub> )	+0.171 (C <sub>ax</sub> 2p' <sub>y</sub> ) +0.206 (O <sub>ax</sub> 2p' <sub>y</sub> )
CC ( $C_2$ ) <sup>b</sup>				
23a'	1	-0.2294	0.132 (H 1s') +0.154d <sub>z<sup>2</sup></sub> -0.469d <sub>x<sup>2</sup></sub> +0.329 (Co s <sub>4</sub> ) +0.389 (Co p <sub>3y</sub> ) -0.182 (C <sub>ax</sub> 2s')	+0.250d <sub>x<sup>2</sup></sub>   +0.224 (Co s <sub>5</sub> ) -0.502 (Co p <sub>3x</sub> ) -0.118 (C <sub>ax</sub> 2p' <sub>x</sub> )
22a'	1	-0.5547	+0.123 (O <sub>ax</sub> 2p' <sub>x</sub> ) -0.122 (C <sub>eq</sub> 2s') -0.111 (O <sub>eq</sub> 2p' <sub>y</sub> ) -0.589d <sub>y<sup>2</sup></sub> +0.202d <sub>z<sup>2</sup></sub>	-0.123 (C <sub>eq</sub> 2p' <sub>z</sub> )   +0.358d <sub>x<sup>2</sup></sub> -0.783d <sub>xy</sub>
21a'	2	-0.3568	-0.189 (Co p <sub>3x</sub> ) -0.255 (H 1s) -0.131d <sub>y<sup>2</sup></sub> +0.157d <sub>xy</sub> -0.298 (Co s <sub>4</sub> ) +0.164 (C <sub>eq</sub> 2s')	-0.452 (H 1s') +0.201d <sub>z<sup>2</sup></sub>   -0.247 (Co p <sub>3x</sub> )
20a'	2	-0.5163	-0.159 (H 1s') +0.702d <sub>y<sup>2</sup></sub> -0.562d <sub>xy</sub>	-0.649d <sub>x<sup>2</sup></sub>
13a''	2	-0.5211	+0.953d <sub>yz</sub>	
12a''	2	-0.5441	0.960d <sub>xz</sub>	

<sup>a</sup>Total energy is -1712.5609 au. <sup>b</sup>Total energy is -1712.5645 au.

**Table XI.** Bond Lengths (Å) and Angles (deg) of the  $^3A''$  Configuration of  $\text{HCo}(\text{CO})_3$ 

parameter	HC ( $C_2$ )	parameter	HC ( $C_2$ )
H-Co	1.66	H-Co-C <sub>ax</sub>	170.2
Co-C <sub>ax</sub>	1.94	H-Co-C <sub>eq</sub>	85.7
Co-C <sub>eq</sub>	2.11	C <sub>ax</sub> -Co-C <sub>ax</sub>	
C <sub>ax</sub> -O <sub>ax</sub>	1.14	C <sub>eq</sub> -Co-C <sub>eq</sub>	119.7
C <sub>eq</sub> -O <sub>eq</sub>	1.12	Co-C <sub>ax</sub> -O <sub>ax</sub>	176.1
		Co-C <sub>eq</sub> -O <sub>eq</sub>	168.3

**Table XII.** Mulliken Charge Distribution on the  $^3A''$  Configuration of  $\text{HCo}(\text{CO})_3$ 

atom	HC ( $C_2$ )	atom	HC ( $C_2$ )
H	-0.272	O <sub>ax</sub>	-0.471
Co	+0.595	C <sub>eq</sub>	+0.423
C <sub>ax</sub>	+0.129	O <sub>eq</sub>	+0.414

by the Mulliken population analysis (Tables II, V, VIII, XII, and XVI). These charges do not correspond to any quantum-mechanical observables and are known to be very dependent on the choice of basis. Hartree-Fock studies of transition-metal carbonyls,<sup>28,29</sup> in somewhat larger basis sets, have attributed negative charge to the metal atom, in contrast with the results presented here (see also ref 7 and the discussion therein). It must be pointed out that, in these studies, diffuse *d*-functions were included in the basis set. The effect of diffuse basis functions, which are indeed indispensable for a good description of the transition-metal compounds,<sup>16,27</sup> is to attribute to a great deal of delocalized charge to the atom on which they are centered. Our own calculations in a larger basis set reduce the charge on the cobalt atoms to ca. +0.1 unit. We conclude that no great significance should be attributed to the absolute values of charges obtained by Mulliken analysis in the presence of diffuse basis functions. Comparisons within the same basis, however, should have more physical meaning, and we see, for example, that a more tightly bound equatorial hydrogen is less negative than the hydride-like axial one (Table II). This is a plausible result, which is also in keeping with earlier studies on the distribution of charge in TBP complexes.<sup>17</sup>

Similarly, we find that the Löwdin population analysis does not provide a description which could be readily compared with that of the Mulliken analysis. As an illustration, we quote the Löwdin charges of the two conformations of  $\text{HCo}(\text{CO})_4$  (Table II). In contrast with the Mulliken charges, and in agreement with the Löwdin charges obtained by an iterative Hückel calculation,<sup>7</sup> the metal atom is negative. The difference between the two population analyses amounts to a gain of ca. 0.9 unit on cobalt, most of the charge being reassigned from the oxygen atoms.

In the simplified case of two atomic orbitals,  $\chi_A$  and  $\chi_B$ , located on the centers A and B, with an electron pair localized entirely in the orbital  $\chi_A$ , Mulliken populations are  $P_A = 2$  and  $P_B = 0$ . Löwdin populations, on the other hand, depend on the overlap,  $\sigma$ , between the two orbitals and are given by:

$$\Pi_A = 1 + (1 - \sigma^2)^{1/2}$$

$$\Pi_B = 1 - (1 - \sigma^2)^{1/2}$$

This indicates that the localized lone pairs, for example, yield substantially smaller Löwdin populations, provided that the atomic orbitals which describe them overlap significantly with the empty orbitals on neighboring centers.

A model SCF calculation on carbon monoxide, in the 3-21G basis, yields an energy of -112.0933 au, a C-O distance of 1.129 Å, and the Mulliken and Löwdin charges of 0.437 and 0.072, respectively (carbon atom carries the positive charge). The loss of 0.365 unit on the carbon atom, and the corresponding gain on oxygen, is due to the different assignment of the  $\sigma$ -type lone-pair charge.

In  $\text{HCo}(\text{CO})_4$ , total loss on the oxygen atoms is 1.635 in the  $C_{3v}$  form and 1.626 in the  $C_{2v}$ , comparable to the total loss of 1.460 units in four free CO's. Total gain on the carbon atoms, in the  $C_{3v}$  form, is only 0.723, implying a loss of 0.728 in the non-CO overlaps. This compares well with the gain of 0.908 unit on cobalt and can be attributed to the difference in description of the carbon lone pairs, which overlap with the valence orbitals on cobalt. In the  $C_{2v}$  form, the carbon loss is 0.732, and the cobalt gain is 0.858 unit.

**EHT Results.** In a number of articles,<sup>17-19</sup> Hoffmann et al. have investigated TBP complexes, by analyzing their (hypothetical) fragments by means of the extended Hückel theory. They found<sup>19</sup> that the  $\text{M}(\text{CO})_4^+$  fragments possess a high-lying  $a_1$ -orbital,  $4p_z + d_{z^2}$ , which is empty in the case of complexes with eight or fewer *d*-electrons and which accepts an electron pair from the hydride

ion. Moreover,  $C_{2v}$  and  $C_{4v}$  geometries of such fragments also have a second, lower lying, filled  $a_1$ -orbital, which interacts with the hydride in a destabilizing manner. The  $C_{3v}$  geometry does not have this second  $a_1$ -orbital and should, therefore, be the preferred geometry in the case of  $\text{HCo}(\text{CO})_4$ .

This description holds fairly well in case of the  $C_{3v}$  configuration of  $\text{HCo}(\text{CO})_4$ . Orbital  $17a_1$  corresponds to the receptor  $a_1$  and can be viewed as a combination of frontier orbitals of the hydride and the  $\text{Co}(\text{CO})_4^+$  fragment. Also, charges on the atoms (Table II) are indicative of a partial hydride nature of this configuration.

Regarding the  $C_{2v}$  configuration, its  $19a_1$ -orbital corresponds to Hoffmann's destabilizing  $a_1$  and is, in fact, a nonbonding orbital:  $\text{H} - d_{x^2-y^2} + 4p_z$ , hybridized away from the hydrogen. Below this orbital lies the bonding  $18a_1$ :  $\text{H} + d_{x^2-y^2} + 4s$ . Formally,  $18a_1$  and  $19a_1$  came about through the interaction of the hydride with an occupied orbital, and the net covalent bonding effect should be zero. However, the charge distribution indicates that the H-Co bond in this conformation is also partially ionic (see Table II).

Hoffmann's argument<sup>19</sup> in favor of the  $C_{3v}$  conformation concentrates entirely on the symmetry-allowed HOMO-LUMO interactions. We find the energy of the  $d_{xy}$ -orbital, as well as that of the supposedly indifferent  $e''$ -like set, to be noticeably lower in the  $C_{2v}$  conformation than in the  $C_{3v}$ , even though they do not overlap with the hydrogen orbitals at all. This lowering compensates for the increase in energy of the orbital  $d_{x^2-y^2}$  due to the interaction with hydrogen. In terms of a simple electrostatic argument, the difference between the two conformations is no more than that of symmetry: the same set of ligands splits the *d*-levels in two different patterns, while preserving the total energy of the *d*-electrons, due to the unchanged total electrostatic repulsion. Moreover, the energy of the unoccupied  $d_{z^2}$ -orbital (not listed in Table III) does not change very much; its value is +0.309 au in the  $C_{3v}$  and +0.305 au in the  $C_{2v}$  conformation. This leads us to expect small energy differences between the two conformations and no distinct correlation between the overall energy and the energy of the highest occupied orbital. We see that such is indeed the case.

In an article preceding the above analysis of the carbonyl fragments, Rossi and Hoffmann<sup>18</sup> provided a detailed account of the  $\sigma$ - and  $\pi$ -bonding effects in TBP complexes and of the relative stability of conformers, which could be inferred from these effects. We summarize here those points of their argument which are relevant to the present study.

In the  $d^8$ -complexes of the TBP type,  $\sigma$ -donating ligands should prefer axial sites to equatorial ones, since the equatorial *d*-orbitals of the  $e'$ -set are occupied, while the axial orbital  $a_1$  is empty. Carbonyl, however, is also a cylindrically symmetrical  $\pi$ -acceptor and should, on that account, prefer an equatorial site. The reason for this preference is the following: in the axial position, a cylindrical acceptor stabilizes both occupied orbitals of the  $e''$ -set equally through the back-bonding interaction. In the equatorial position (e.g., along the *x* axis), interaction with the  $d_{xz}$ -orbital remains unchanged while that with the  $d_{yz}$ -orbital is prohibited by symmetry. Instead, the ligand interacts with the  $d_{xy}$ -member of the  $e'$ -set. This interaction is stronger than that with the  $d_{yz}$ -orbital, due to the hybridization of the  $e'$ -set with the *4p*-orbitals of the metal atom, resulting in a preference for the equatorial site.

It would be difficult to draw definite conclusions from this argument regarding the stability of conformations of the  $\text{HCo}(\text{CO})_4$  compound, mostly because of the opposing tendencies of the carbonyl ligand. However, it is instructive to compare the above predictions with the calculated energies of the *d*-electrons in the two geometries.

We see from Table III that the  $e''$ -set follows the predictions: energy of the  $d_{xz}$ -orbital differs slightly from one geometry to the other (0.008 au), while the  $d_{yz}$  appears to be somewhat stabilized by the axial carbonyl (0.019 au). The small but distinct orbital contributions, due to back-bonding, were omitted from Table III.

The orbital  $d_{xy}$ , however, has lower energy in the  $C_{2v}$  conformation (0.054 au), despite loss of  $\pi$ -bonding with one equatorial carbonyl. Its mixing with the  $4p_z$  metal orbital also decreases in the  $C_{2v}$  case, which, along with an increase in the angle between

(17) Hoffmann, R.; Howell, J. M.; Muetterties, E. L. *J. Am. Chem. Soc.* **1972**, *94*, 3047.

(18) Rossi, A. R.; Hoffmann, R. *Inorg. Chem.* **1975**, *14*, 365.

(19) Elian, M.; Hoffmann, R. *Inorg. Chem.* **1975**, *14*, 1058.

(20) Sweeny, R. L. *J. Am. Chem. Soc.* **1982**, *104*, 3739.

the equatorial ligands ( $132.4^\circ$ ), leads us to believe that the stabilization of this orbital is mostly due to diminished electrostatic repulsion. Naturally, this effect is much smaller in the orbitals of the  $e''$ -set, allowing the covalent stabilization to come to the fore.

In the light of these considerations, we conclude that the arguments based on the HOMO–LUMO interaction of fragments described by the Hückel theory are overly simplistic and certainly inadequate to rationalize the energetics of transition-metal complexes. One obvious drawback of such analyses is, of course, the absence of even a qualitative description of the Coulomb interactions.

From a practical standpoint, small energy differences (of the order of 0.001 au) require *ab initio* calculations more detailed even than the present one, in order to resolve the question of the relative stability of conformations.

It is interesting to note, however, that the description of the frontier orbitals remains roughly comparable in EHT and *ab initio* methods, indicating that the former might be entirely adequate for a qualitative description of processes such as  $C_{2v}$  and  $C_{3v}$  rearrangements.

**Comparison with the Experimental Results and the Problem of Bond Lengths.** Experimental values<sup>2</sup> of the bond lengths and angles of the  $C_{3v}$  conformation of  $HCo(CO)_4$ , obtained by electron diffraction in the gas phases, are listed in Table I. These data compare well with earlier X-ray diffraction results<sup>21</sup> on the iso-electronic anion  $[HFe(CO)_4]^-$ , whose geometry should be similar to that of  $HCo(CO)_4$ .

The most obvious discrepancy between the theoretical and experimental geometries lies in the cobalt–ligand bond lengths. The theoretically predicted values are consistently too large, a well-known difficulty in the *ab initio* treatment of transition-metal complexes.<sup>22–25</sup> All of the fully optimized geometries of hydridocobalt tri- and tetracarbonyls reported so far<sup>5,8,9</sup> were obtained by means of semiempirical methods, which fare somewhat better with respect to the bond lengths. However, one study<sup>5</sup> shows that considerable readjustment of the MEHT parameters is necessary, in order to bring the H–Co distance down to an experimentally justifiable level.

Studies of the geometries of metallocenes<sup>23–25</sup> at the Hartree–Fock level yielded metal–ring distances considerably larger than the experimentally observed ones. A systematic enlargement of the basis set on the ferrocene<sup>24</sup> provided no more than a marginal improvement of the bond length, with no indication that the remaining error (ca. 14%) could be corrected by expanding the basis set further. These studies indicate strongly that the excessive metal–ligand bond lengths represent a correlation effect which, at present, cannot be easily included into the optimization of the geometry of transition-metal complexes.

A related study<sup>26</sup> of iron pentacarbonyl provides a good illustration of the dependence of bond lengths and force constants on the electron correlation, as well as of the computational difficulties involved.

### Structure of the Tricarbonyl Compound

By following the pattern of the distorted TBP structure, and treating a vacancy as tantamount to a ligand, one can postulate four sterical conformations for the hydridocobalt tricarbonyl. We label these conformations by the ligands in apical positions, which

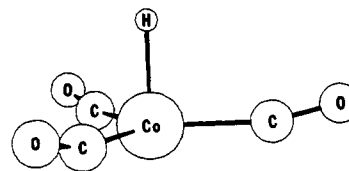


Figure 3. HV conformation of  $HCo(CO)_3$ ,  $^1A_1$ .

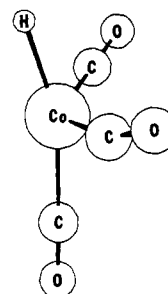


Figure 4. HC conformation of  $HCo(CO)_3$ ,  $^1A'$ .

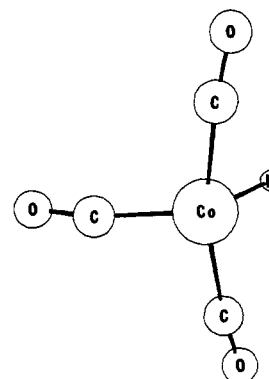


Figure 5. CC conformation of  $HCo(CO)_3$ ,  $^1A'$ .

Table XIII. Mulliken Spin Population on the  $^3A''$  Configuration of  $HCo(CO)_3$

atom	HC ( $C_s$ )	atom	HC ( $C_s$ )
H	−0.001	O <sub>ax</sub>	0.125
Co	1.528	C <sub>eq</sub>	0.021
C <sub>ax</sub>	0.282	O <sub>eq</sub>	0.011

is sufficient to characterize them.

**HV (Hydrogen–Vacancy):** highest possible symmetry  $C_{3v}$ . This structure was predicted by Grima et al.<sup>8</sup> by means of CNDO/2. They also studied the HC conformation and apparently did not find it to be a distinct minimum on the energy surface.

**HC (Hydrogen–Carbon):** highest possible symmetry  $C_s$ . This conformation, along with HV, was predicted by Bellagamba et al.<sup>6</sup> using the EHT technique. HC was found to be more stable than HV.

**CC (Carbon–Carbon):** highest symmetry  $C_s$ .

**CV (Carbon–Vacancy):** highest symmetry  $C_s$ .

An INDO/1 study of Iberle and Davidson<sup>9</sup> found the structures HV and CC to constitute distinct energy minima. To the authors' knowledge, the CV conformation has not been described in the literature.

The notion that all geometries of  $HCo(CO)_3$  could be derived from the TBP is a plausible guess but not a proven fact. Distortions of the tetrahedron are also acceptable, and Elian and Hoffmann<sup>19</sup> provide a theoretical argument in favor of the tetrahedral geometry for triplet states. We used TBP-derived conformations as initial guesses in the geometry optimizations, while taking care not to prejudice the outcome with unwarranted symmetry constraints. Our calculations have confirmed the TBP hypothesis in all closed-shell cases.

**Closed-Shell States of  $HCo(CO)_3$ .** We have carried out geometry optimizations of the four conformations of  $HCo(CO)_3$ ,

(21) Smith, M. B.; Bau, R. *J. Am. Chem. Soc.* **1973**, *95*, 2388.

(22) Demuyneck, J.; Strich, A.; Veillard, A. *Nouv. J. Chim.* **1977**, *1*, 217.

(23) Luthi, H. P.; Ammeter, J.; Almlof, J.; Korsell, K. *Chem. Phys. Lett.* **1980**, *69*, 540.

(24) Luthi, H. P.; Ammeter, J. H.; Almlof, J.; Faegri, K. *J. Chem. Phys.* **1982**, *77*, 2002.

(25) Almlof, J.; Faegri, K.; Schilling, B. E. R.; Luthi, H. P. *Chem. Phys. Lett.* **1984**, *106*, 266.

(26) Luthi, H. P.; Siegbahn, P. E. M.; Almlof, J. *J. Phys. Chem.* **1985**, *89*, 2156.

(27) Hay, P. J. *J. Chem. Phys.* **1977**, *66*, 4377.

(28) Hay, P. J. *J. Am. Chem. Soc.* **1978**, *100*, 2411.

(29) Kirschenbaum, L. J.; Howell, J. M.; Rossi, A. R. *J. Phys. Chem.* **1981**, *85*, 17.

**Table XIV.** Frontier Orbitals of the  $^3A''$  Configuration of  $HCo(CO)_3$ 

orbital	occu- pation	energy, au	main components of orbital	
24a'	1	-0.2161	HC ( $C_s$ ) <sup>a</sup>	
			0.175d <sub>x<sup>2</sup></sub>	-0.341d <sub>z<sup>2</sup></sub>
			+0.160d <sub>y<sup>2</sup></sub>	
			+0.142 (Co s <sub>4</sub> )	+0.165 (Co s <sub>5</sub> )
			+0.532 (Co p <sub>3x</sub> )	-0.129 (Co p <sub>3z</sub> )
12a''	1	-0.5879	+0.255 (C <sub>ax</sub> 2p <sub>x</sub> )	+0.378 (C <sub>ax</sub> 2p' <sub>x</sub> )
			-0.121 (C <sub>ax</sub> 2s')	-0.334 (O <sub>ax</sub> 2p' <sub>x</sub> )
			-0.213 (O <sub>ax</sub> 2p <sub>x</sub> )	-0.169 (Co p <sub>3y</sub> )
			-0.978d <sub>xy</sub>	-0.480 (H 1s')
			-0.263 (H 1s)	-0.209d <sub>z<sup>2</sup></sub>
23a''	2	-0.3691	+0.116d <sub>x<sup>2</sup></sub>	-0.291 (Co p <sub>3z</sub> )
			-0.186 (Co s <sub>4</sub> )	
			+0.162 (C <sub>eq</sub> 2s')	
			-0.809d <sub>x<sup>2</sup></sub>	+0.759d <sub>y<sup>2</sup></sub>
			+0.235d <sub>zz</sub>	-0.144 (Co s <sub>4</sub> )
22a'	2	-0.5368	+0.122 (C <sub>ax</sub> 2s')	
			-0.287d <sub>x<sup>2</sup></sub>	+0.122d <sub>z<sup>2</sup></sub>
			+0.171d <sub>y<sup>2</sup></sub>	-0.871d <sub>zz</sub>
			-0.164 (C <sub>ax</sub> 2s')	
			-0.125 (O <sub>ax</sub> 2p <sub>x</sub> )	-0.152 (O <sub>ax</sub> 2p' <sub>x</sub> )
11a''	2	-0.5709	+0.865d <sub>yz</sub>	

<sup>a</sup>Total energy is -1712.5598 au.**Table XV.** Bond Lengths (Å) and Angles (deg) of the Tetrahedral Conformations of  $HCo(CO)_3$ 

parameter	$C_{3v}$	$C_s (e')^1(t_2')^1$	$C_s (e'')^1(t_2'')^1$
H-Co	1.61	1.62	1.61
Co-C <sub>x</sub>	2.03	1.94	2.10
Co-C <sub>y</sub>		2.19	2.15
C <sub>x</sub> -O <sub>x</sub>	1.13	1.12	1.13
C <sub>y</sub> -O <sub>y</sub>		1.12	1.12
H-Co-C <sub>x</sub>	114.6	123.7	114.1
H-Co-C <sub>y</sub>		109.7	113.1
C <sub>x</sub> -Co-C <sub>y</sub>	103.9	99.1	109.2
C <sub>y</sub> -Co-C <sub>y</sub>		115.3	96.9
Co-C <sub>x</sub> -O <sub>x</sub>	169.6	171.3	175.5
Co-C <sub>y</sub> -O <sub>y</sub>		169.7	170.9

**Table XVI.** Mulliken Charge Distribution on the Tetrahedral Conformations of  $HCo(CO)_3$ 

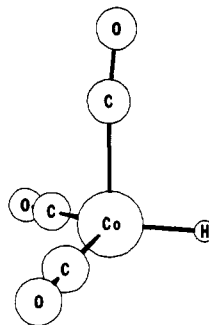
atom	$C_{3v}$	$C_s (e')^1(t_2')^1$	$C_s (e'')^1(t_2'')^1$
H	-0.156	-0.164	-0.144
Co	+0.379	+0.284	+0.196
C <sub>x</sub>	+0.356	+0.297	+0.408
O <sub>x</sub>	-0.431	-0.442	-0.423
C <sub>y</sub>		+0.426	+0.404
O <sub>y</sub>		-0.413	-0.423

**Table XVII.** Mulliken Spin Population on the Tetrahedral Conformations of  $HCo(CO)_3$ 

atom	$C_{3v}$	$C_s (e')^1(t_2')^1$	$C_s (e'')^1(t_2'')^1$
H	0.000	0.000	0.000
Co	1.983	1.970	1.972
C <sub>x</sub>	0.004	0.004	0.006
O <sub>x</sub>	0.001	0.001	0.004
C <sub>y</sub>		0.009	0.007
O <sub>y</sub>		0.003	0.001

constraining the symmetry to  $C_{3v}$  or  $C_s$  and assuming a closed-shell electron configuration. In contrast with the results of other authors,<sup>6,9</sup> we found all conformations to be true minima on the SCF energy surface.

Additional, unconstrained optimizations were performed, in order to check for distortions to lower symmetry, but none were found. Results of the geometry optimizations are listed in Table IV. For the purpose of simplicity, we have omitted the dihedral angles of the equatorial carbonyls in  $C_s$  conformations. In general, carbonyl oxygens are tilted some 10–15° toward the hydrogen atom; their exact orientation does not seem to matter very much.

**Figure 6.** CV conformation of  $HCo(CO)_3$ ,  $^1A'$ .**Table XVIII.** Frontier Orbitals of the Tetrahedral Conformations of  $HCo(CO)_3$ 

orbital	occu- pation	energy, au	main components of orbital	
11e	1	-0.4868	$C_{3v}$ <sup>a</sup>	
			0.555d <sub>xy</sub>	+0.789d <sub>yz</sub>
	1	-0.4868	+0.222 (Co p <sub>3y</sub> )	
			-0.481d <sub>x<sup>2</sup></sub>	+0.481d <sub>y<sup>2</sup></sub>
13a <sub>1</sub>	2	-0.2909	+0.789d <sub>zz</sub>	+0.222 (Co p <sub>3x</sub> )
			-0.176 (H 1s)	-0.159 (H 1s')
			-0.259d <sub>x<sup>2</sup></sub>	-0.259d <sub>y<sup>2</sup></sub>
			+0.500d <sub>z<sup>2</sup></sub>	
12a <sub>1</sub>	2	-0.4205	-0.179 (Co s <sub>4</sub> )	-0.501 (Co p <sub>3z</sub> )
			-0.197 (H 1s)	-0.441 (H 1s')
10e	2	-0.4281	+0.373d <sub>x<sup>2</sup></sub>	+0.373d <sub>y<sup>2</sup></sub>
			-0.711d <sub>z<sup>2</sup></sub>	-0.137 (Co s <sub>4</sub> )
	2	-0.4281	0.664d <sub>x<sup>2</sup></sub>	-0.664d <sub>y<sup>2</sup></sub>
			+0.567d <sub>zz</sub>	
24a'	1	-0.4609	$C_s (e')^1(t_2')^1$ <sup>b</sup>	
			-0.459d <sub>x<sup>2</sup></sub>	+0.816d <sub>y<sup>2</sup></sub>
23a'	1	-0.4973	-0.335d <sub>z<sup>2</sup></sub>	+0.521d <sub>zz</sub>
			+0.199 (Co p <sub>3x</sub> )	
22a'	2	-0.2916	-0.304d <sub>x<sup>2</sup></sub>	-0.201d <sub>x<sup>2</sup></sub>
			+0.534d <sub>y<sup>2</sup></sub>	-0.828d <sub>zz</sub>
			+0.144 (Co p <sub>3z</sub> )	
			-0.188 (H 1s)	-0.195 (H 1s')
12a''	2	-0.3869	-0.429d <sub>x<sup>2</sup></sub>	+0.421d <sub>z<sup>2</sup></sub>
			-0.198 (Co s <sub>4</sub> )	-0.113 (Co s <sub>5</sub> )
21a''	2	-0.4038	-0.458 (Co p <sub>3z</sub> )	-0.489d <sub>yz</sub>
			-0.787d <sub>xy</sub>	
11a''	2	-0.4099	+0.265 (Co p <sub>3z</sub> )	
			-0.183 (H 1s)	-0.424 (H 1s')
			+0.619d <sub>x<sup>2</sup></sub>	-0.674d <sub>z<sup>2</sup></sub>
			-0.501d <sub>xy</sub>	+0.822d <sub>yz</sub>
12a''	1	-0.5003	$C_s (e'')^1(t_2'')^1$ <sup>c</sup>	
			-0.827d <sub>xy</sub>	-0.520d <sub>yz</sub>
11a''	1	-0.5297	-0.176 (Co p <sub>3y</sub> )	
			0.524d <sub>xy</sub>	-0.839d <sub>yz</sub>
24a''	2	-0.2719	-0.158 (H 1s)	
			-0.418d <sub>xi</sub>	-0.135d <sub>y<sup>2</sup></sub>
			+0.527d <sub>z<sup>2</sup></sub>	
			-0.125 (Co s <sub>4</sub> )	-0.547 (Co p <sub>3z</sub> )
23a'	2	-0.3785	0.146 (H 1s)	+0.312 (H 1s')
			-0.624d <sub>x<sup>2</sup></sub>	+0.277d <sub>y<sup>2</sup></sub>
			+0.328d <sub>z<sup>2</sup></sub>	+0.488d <sub>zz</sub>
			+0.146 (Co s <sub>4</sub> )	+0.236 (Co p <sub>3x</sub> )
22a'	2	-0.4011	0.127 (H 1s)	+0.288 (H 1s')
			-0.301d <sub>x<sup>2</sup></sub>	-0.117d <sub>y<sup>2</sup></sub>
			+0.386d <sub>z<sup>2</sup></sub>	-0.753d <sub>zz</sub>
			+0.116 (Co s <sub>4</sub> )	-0.163 (Co p <sub>3x</sub> )
21a'	2	-0.4500	-0.189 (H 1s')	
			-0.415d <sub>x<sup>2</sup></sub>	+0.885d <sub>y<sup>2</sup></sub>
			-0.464d <sub>z<sup>2</sup></sub>	-0.307d <sub>zz</sub>

<sup>a</sup>Total energy is -1712.6045 au. <sup>b</sup>Total energy is -1712.5910 au.<sup>c</sup>Total energy is -1712.5832 au.

Figures 3–6 show the geometries of the closed-shell states of  $HCo(CO)_3$ .

Table VI summarizes the electronic features of the four conformations. Again, one finds an  $e''$ -like set of pure d-orbitals, as

well as an  $e'$ -like set, mixing the 4s- and 4p-orbitals. In this molecule, however, distortions from the TBP structure are complicated by the absence of a carbonyl ligand.

While the LUMOs of the tetracarbonyl do not have special significance, the lowest empty orbital of every closed-shell, TBP-derived form of the tricarbonyl is an spd hybrid, directed toward the vacant site. Such orbitals have been described for similar complexes by Elia and Hoffmann<sup>19</sup> at the EHT level. This acceptor orbital would account for the postulated readiness of the tricarbonyl to accept a fourth carbonyl ligand.<sup>20</sup>

An interesting aspect of the LUMO is the role of the ligand orbitals: p- and sp-orbitals on the carbon atoms overlap sideways with the central lobe on the metal, extending the LUMO over an entire side of the molecule. It is not clear whether this should have any effect upon the reactivity of  $\text{HCo}(\text{CO})_3$ .

The manner in which hydrogen is bound to cobalt is essentially the same as in the tetracarbonyl molecule; in the apical case, an axial spd hybrid forms the bond to hydrogen, and in the equatorial case, one of the  $e'$ -orbitals interacts, forming the bond and a high-lying  $e'$ -like antibonding orbital. H-Co bond lengths are distinctly different in the apical and equatorial cases and comparable to their counterparts in tetracarbonyl (see Tables II and IV).

There are also distinct gaps (0.03–0.05 au) in the  $e''$ -like orbital sets of the conformations HC and CC, due to the large deviation from the 3-fold axis in these two cases. In the HC case, noticeable rearrangement of both  $e'$ - and  $e''$ -like sets takes place, moving the d-electron distribution away from the carbonyls and toward the vacancy.

**Triplet States of  $\text{HCo}(\text{CO})_3$ .** In their EHT analysis of the fragments of carbonyl complexes, Elia and Hoffmann<sup>19</sup> point out cases in which the change in multiplicity is accompanied by a substantial change in molecular geometry. In particular, a  $C_{3v}$  tetracarbonyl fragment exhibits two  $e$ -levels and an  $a_1$ -level, whose relative positions change with the variation of the angle between apical and basal ligands. The low-lying  $e''$ -like level is fairly insensitive to the change of angle. The upper levels, an  $e'$ -like level and the  $a_1$ , intersect at tetrahedral geometry, forming the  $t_2$ -level of the  $T_d$  symmetry. At smaller angles,  $a_1$  lies above  $e'$ , and the reverse is true for angles greater than tetrahedral. It follows from the building-up principle, and Hund's rule, that a  $d^8$ -complex should have the closed-shell singlet configuration at angles below  $109^\circ$  and a triplet configuration at angles above that value.

We have performed analogous calculations on the  $C_{3v}$  form of  $\text{HCo}(\text{CO})_3$ , by means of the IEHT procedure, which confirmed the results of Elia and Hoffmann. The replacement of the apical carbonyl with hydrogen did not introduce any qualitative changes into the picture. We also notice that our ab initio results for the HV conformation of  $\text{HCo}(\text{CO})_3$  do not contradict the predictions of this simpler theory for the closed-shell case.

Taking into account the possibility of an open-shell ground state for the tricarbonyl, we performed a series of single-double CI calculations at all four TBP geometries, using the closed-shell orbitals obtained by the SCF procedure. This turned up a number of triplet states: geometry optimizations at the open-shell Hartree-Fock SCF level were performed for the triplets of lowest CI energy. Most optimizations were done under the constraint of  $C_s$  symmetry; a few that were not constrained yielded  $C_s$  structures all the same.

Of the TBP-derived geometries, only two were found to be distinct triplet energy minima: HC and CC. Even though the initial geometries were always of the TBP variety, optimizations of HV and CV settled for distorted tetrahedral structures, obliterating the distinction between the apical and equatorial hydrogen. Moreover, HC and CC were found to be  $d^7p^1$ -species, while the tetrahedral conformations are of the  $d^8$  type, similar to the variety described by Elia and Hoffmann. Tables VII–XVIII summarize the results obtained for triplet states of  $\text{HCo}(\text{CO})_3$ .

In the case of the HC conformation, two triplet states are considered:  $^3A'$  and  $^3A''$ . There is some difference in the geometry of these two states (mainly in the bond angles) and an energy

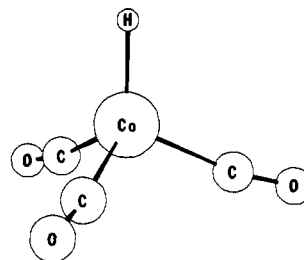


Figure 7.  $C_{3v}$  tetrahedral conformation of  $\text{HCo}(\text{CO})_3$ ,  $^3A_2$ .

difference of 0.001 au, in favor of  $^3A'$ . This energy difference is entirely inconclusive and must be resolved through more accurate calculations. For the time being, we shall treat these two states as equally good candidates for the electronic ground state of this conformation.

One of the unpaired electrons resides in an orbital which is mostly cobalt 4p in character, along with some contribution from p-orbitals on the axial carbonyl. This orbital is obviously related to the low-lying acceptor observed in the closed-shell case. Mulliken spin population analysis places about 50% of one unpaired electron onto the axial carbonyl (see Tables IX and XIII).

The other unpaired electron occupies a metal d-orbital, either  $d_{x^2-y^2}$  in the  $^3A'$ -state or  $d_{xy}$  in the  $^3A''$ -state. There is less electron density placed between equatorial ligands in the latter case, a fact which would account for a smaller angle between equatorial carbonyls in the  $^3A''$ -state (see Tables VII and XI).

In the CC case, there appears to be only one low-lying triplet state:  $^3A'$ . Again, one of the unpaired electrons is placed into the acceptor orbital, which is still largely a directional p-hybrid but with more metal s- and d-character. We see from the population analysis that only about 20% of one unpaired electron is delocalized over the carbonyls (Table IX).

Special attention must be paid to the tetrahedral conformations, of which three were found: one tetrahedron distorted to symmetry  $C_{3v}$  and two to  $C_s$ . All of the tetrahedral conformations are  $d^8$ -species, with unpaired electrons largely of d-character localized almost entirely on the cobalt atom. Again, the  $C_{3v}$  form was reoptimized without constraints, but no deviations from  $C_{3v}$  symmetry were found. Tables XV–XVIII summarize the results obtained for these conformations, and Figure 7 shows the geometry of the  $C_{3v}$  form.

A word should be said about the cobalt-hydrogen bond in the tetrahedral conformations. The EHT analysis<sup>19</sup> of the  $\text{Co}(\text{CO})_3^+$  fragment with eight d-electrons decidedly favors the closed-shell configuration of  $\text{HCo}(\text{CO})_3$ , at the pyramidal angle of  $90^\circ$ . This form of the fragment has all eight d-electrons placed into orbitals of e-symmetry and features a low-lying  $a_1$ -acceptor, ready to form a bond with the hydride ion. At the tetrahedral angle, however, the low  $a_1$ -orbital is filled, and two unpaired electrons populate the higher e-level. There is only a high  $a_1$ -acceptor available to form a bond to hydrogen, and this bond should be destabilized through the interaction with the lower, filled  $a_1$ .

Our results indicate that the electronic structure of these forms of  $\text{HCo}(\text{CO})_3$  can be understood in terms of the level splitting in tetrahedral complexes. It can be seen from Table XVIII that the d-orbitals form an e-like group, directed toward the edges of the tetrahedron, and a  $t_2$ -like group, directed toward the vertices. We shall label the orbitals of these groups as primed or doubly primed, with respect to the reflection in the xz plane.

In all three conformations, one doubly occupied  $t_2$ -orbital interacts with the hydride, and the resulting antibonding combination is hybridized away from the hydrogen by mixing with the metal 4p<sub>z</sub>-orbital. This bonding scheme resembles that of the equatorial H-Co bond in the TBP structures, and the bond length (ca. 1.6 Å) is close to the length of TBP equatorial bonds. At the present level of computation, we cannot conclude that this bond should be any weaker than the apical H-Co bond found in the closed-shell TBP varieties of  $\text{HCo}(\text{CO})_3$ .

Among the tetrahedral conformations,  $C_{3v}$  is the one lowest in energy, 0.013 au below the next higher state. As expected, the



unpaired electrons,  $(t_2')^1(t_2'')^1$ , face the carbonyl ligands, occupying those orbitals of the  $t_2$ -like set which remain unperturbed by the bond to hydrogen. The symmetry of this electronic state is  $^3A_2$ ; Jahn-Teller effects of the first order are, therefore, ruled out. One would also expect to find a similar  $(e')^1(e'')^1$   $^3A_2$ -state of higher energy.

In order to rationalize the two  $C_s$  forms, we notice that, besides the above  $^3A_2$ -states, there are also four "Hückel degenerate" configurations of the type  $(e)^1(t_2)^1$ . These configurations give rise to states  $^3A_1$ ,  $^3A_2$ , and  $^3E$ , the last one being Jahn-Teller unstable in the first order. Also, distortions of the second-order cannot be ruled out, because of the expected proximity of these states.

In general, symmetry distortions tend to maximize the "distance" between the unpaired electrons, and such is the case with both  $C_s$  conformations: the  $(e')^1(t_2')^1$  configuration is distorted by an increase in the angle between hydrogen and the in-plane carbonyl, and the  $(e'')^1(t_2'')^1$  configuration decreases the angle between the out-of-plane carbonyls (see Table XV).

However, single-configuration methods cannot describe the two-determinantal states of the  $C_{3v}$  conformation, and we do not attempt to characterize the two  $C_s$  forms as distortions of any specific states of the full symmetry.

### Summary and Conclusions

In contrast with the earlier studies, our work confirms, as distinct energy minima, all of the sterically plausible TBP conformations of the closed-shell form of the hydridocobalt tri- and

tetracarbonyls. We find that two fairly different bonding schemes apply to the apical and equatorial hydrogen and that the features of the H-Co bond, as well as the d-orbital splitting, cannot be adequately explained by means of Hückel-type methods.

We come across two classes of triplet states of the tricarbonyl compound: there are tetrahedral  $d^8$ -states, similar to those described by Elian and Hoffmann,<sup>19</sup> but we also find the TBP-derived  $d^7p^1$ -states. Unlike the tetrahedral states, those of the second class are closely related to the corresponding closed-shell states: one of the unpaired electrons occupies the directional receptor orbital which appeared in lieu of the missing carbonyl, the concomitant differences between the singlet and triplet geometries being fairly small.

We do not regard the relative energies obtained in this work as conclusive. This is especially true of the comparison between open- and closed-shell states, which would be rather meaningless without taking into account the correlation contributions.

The difficult problem of metal-ligand bond lengths also needs to be explored further. Results of some preliminary CI calculations on the  $HCo(CO)_4$  molecule confirm the hypothesis that this effect is essentially due to the electron correlation.

**Acknowledgment.** This material is based upon work supported by the National Science Foundation under Grants CHE-83-09446, CHE-84-05851, and CHE-85-03415. We also acknowledge the NSF support for the calculations done on the Cyber 205 super-computer at Purdue University in West Lafayette, IN.

## Theoretical Analysis of Hydrocarbon Properties. 1. Bonds, Structures, Charge Concentrations, and Charge Relaxations

Kenneth B. Wiberg,\*<sup>†</sup> Richard F. W. Bader,\* and Clement D. H. Lau

Contribution from the Departments of Chemistry, Yale University, New Haven, Connecticut 06511, and McMaster University, Hamilton, Ontario, L8S 4M1 Canada. Received July 11, 1986

**Abstract:** A theoretical analysis of properties of eight alkanes, four cycloalkanes, seven bicycloalkanes, four propellanes and cubane, tetrahedrane, and spiropentane is presented, based on properties of charge distributions derived from 6-31G\* wave functions. Molecular structures are assigned, and a bridgehead bond is found to be present in each of the propellanes. The shortcomings of using density deformation maps or selected sets of orbitals to assign a molecular structure are discussed. Bonds are characterized in terms of a bond order, a bond ellipticity, and the differing extents to which charge is locally concentrated and depleted as determined by the Laplacian of  $\rho$ . Bond orders range from 0.7 to 1.3 in the propellanes. Ellipticities of bonds in three-membered rings—a measure of the tendency for charge density to be preferentially accumulated in a given plane—are found to exceed that for the double bond in ethylene. This property and the Laplacian of  $\rho$  are used to account for the relative reactivities and structural stabilities of molecules containing small rings. The difference between the bond angle and the corresponding angle formed by bond paths provides a measure of the degree of relaxation of the charge density away from the geometrical constraints imposed by the nuclear framework. The bond path angle is found to exceed the geometrical angle by 23° in spiropentane, 21° in tetrahedrane, 19° in cyclopropane, and -1.5° in cyclohexane. The lowest energy transition densities in the propellanes are used to describe the charge reorganizations accompanying the most facile of the nuclear motions in these molecules.

### I. Introduction

The small ring propellanes such as [1.1.1]propellane have unusual structures with "inverted" tetrahedral geometries at the bridgehead carbon atoms, giving them unusual properties and chemical reactivities.<sup>1</sup> We should like to obtain a theoretical understanding of the differences between the properties of these compounds and those of other cyclic hydrocarbons. It has been demonstrated that ab initio molecular orbital calculations are capable of satisfactorily predicting the geometries,<sup>2</sup> enthalpies of

formation,<sup>3</sup> vibrational and photoelectron spectra,<sup>4,5</sup> and dipole moments of hydrocarbon molecules in general and of the cyclic

(1) Wiberg, K. B. *Acc. Chem. Res.* **1985**, *17*, 379.

(2) Pople, J. *Mod. Theor. Chem.* **1977**, *4*, 1. Hehre, W. J.; Radom, L.; Schleyer, P. v. R.; Pople, J. *Ab Initio Molecular Orbital Theory*; Wiley: New York, 1986.

(3) (a) Wiberg, K. B. *J. Comput. Chem.* **1984**, *5*, 197. (b) Wiberg, K. B. *J. Org. Chem.* **1985**, *50*, 5285. (c) Ibrahim, M. R.; Schleyer, P. v. R. *J. Comput. Chem.* **1985**, *6*, 157.

(4) Pople, J. A.; Schlegel, H. B.; Krishnan, R.; DeFrees, D. J.; Binkley, J. S.; Frisch, M. J.; Whiteside, R. A.; Hart, R. F.; Hehre, W. J. *Int. J. Quantum Chem., Quantum Chem. Symp.* **1981**, *15*, 269. Hess, B. A., Jr.; Schaad, L. J.; Carsky, P.; Zahradnik, R. *Chem. Rev.* **1986**, 709-762.

<sup>†</sup> Yale University.